Extension of the Stream of Variation Model for General Purpose Workholding Devices: Vices and 3-jaw Chucks

Rubén Moliner-Heredia, José Vicente Abellán-Nebot, Ignacio Peñarrocha-Alós

***Abstract*—Nowadays, advanced manufacturing models such as the Stream-of-Variation (SoV) model have been successfully applied to derive the complex relationships between fixturing, manufacturing and datum errors throughout a multi-stage machining process. However, the current development of the SoV model is still based on 3-2-1 fixturing schemes and, although some improvements have been done, e.g. N-2-1 fixtures, the effect of general workholding systems such as bench vices or 3-jaw chucks has not yet been included into the model.**

This paper presents the extension of the SoV model to include fixture and datum errors considering both bench vices and 3-jaw chucks as a fixturing devices in multi-stage machining processes. The model includes different workholding configurations and it is shown how to include the workholding accuracy to estimate part quality. The extended SoV model is validated in a 3-stage machining process by both machining experimentation and CAD simulations.

Note to Practitioners: ***Abstract*—Part quality estimation in multi-stage machining systems is a challenging issue. The Stream of Variation (SoV) model is a straightforward model that can be used for this purpose. However, current model is limited to fixture based on punctual locators and common shop-floor devices are not considered yet. To overcome this limitation, this paper extends the current SoV model to include vices and 3-jaw chucks as workholding devices. The proposed methodology let practitioners to estimate the manufacturing capability of a process considering the technical specifications of these devices (e.g., paralelism and perpendiculary of vice surfaces, total indicator runout of chucks) or it can be used for diagnosing workholding issues. The model assumes that the workpiece acts as a rigid part and errors due to deformation during clamping are assumed to be negligible in comparison with fixture- and datum-induced errors.**

***Index Terms*—Stream of Variation, fixturing errors, workholding, multi-stage manufacturing process.**

I. Nomenclature

^{0}FCS, FCS	Nominal and actual fixture coordinate system
${}^0\mathbf{H}_F^R$, $\mathbf{H}_F^R$	Nominal and actual Homogeneous Transformation Matrix (HTM) between RCS and FCS
$\mathbf{\Delta}_F^R$, $\delta\mathbf{H}_F^R$	Differential and deviation transformation matrix between RCS and FCS
$\mathbf{x}_F^R$	DMV representing the deviation of FCS in RCS.
$\mathbf{d}_F^R$, $\boldsymbol{\theta}_F^R$	Position and orientation deviation of FCS with respect to (w.r.t.) RCS
$\mathbf{t}_F^R$, $\boldsymbol{\omega}_F^R$	Position and orientation vector of FCS w.r.t. RCS
$\hat{\boldsymbol{\theta}}_F^R$	Skew symmetric matrix from $\boldsymbol{\theta}_F^R$
$\mathbf{x}_k$	Vector with the DMV of all features stacked up at stage k
$\mathbf{u}_k^f$	Fixture errors at stage k
$\mathbf{A}_k^3$	Fixture-induced variation matrix in SoV model
$\mathbf{A}_k^2$	Datum-induced variation matrix in SoV model

R. Moliner-Heredia, J.V. Abellán-Nebot and I. Peñarrocha-Alós are with the Departament of Industrial Systems Engineering and Design, Universitat Jaume I, Castellón de la Plana, Spain.

II. Introduction

MANUFACTURING processes have to be environmental friendly and safe and deliver high quality products rapidly adapted to customer requirements at a minimum cost. One of the most important challenges in modern industry is the implementation of manufacturing systems capable of generating products with zero defects. A recent roadmap promoted by the European Comission in the research area of zero-defect manufacturing processes has presented the state of the art, the gap to be overcome and the research priorities and future trends in this field [1]. According to the roadmap, a research priority for the development of zero-defect manufacturing processes is related to the "integration of machine, fixture, tool and workpiece models for quality and resource deterioration prediction" in multi-stage manufacturing processes (MMPs).

MMPs are manufacturing processes that consist of a sequence of stages where manufacturing operations such as assembly or machining operations are sequentially conducted to manufacture a part or product. Typical examples of MMPs are automobile body assembly processes and multi-job machining processes where a part moves from one stage to another until a semi-finished or finished product is obtained. Due to the sequential nature of these manufacturing operations, the error generated at the first stages may be propagated downstream to other stages which produces additional manufacturing errors. These complex error interactions make difficult to control product quality and tasks such as predictive maintenance, process control, quality assurance and fault diagnosis are challenging.

In order to illustrate the error propagation in a MMP, consider a MMP composed of 3 stages in a machining line as shown in Figure 1. As it can be observed, stage 1 presents a deviation of the cutting-tool trajectory, producing a machining-induced error. The resulting part moves to stage 2, where

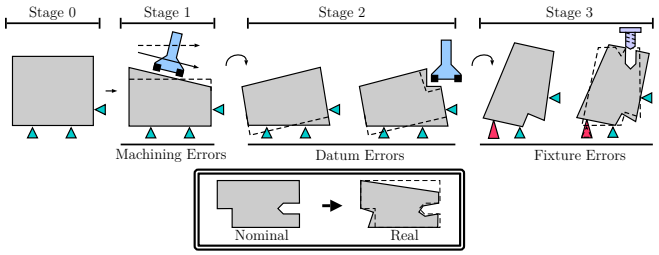

Fig. 1: Error transmission in Multi-stage Manufacturing Processes (MMP).

there are no additional errors. However, since the previous machined surface is used as a datum surface, the square shoulder machining operation is deviated with respect to the top surface, producing a datum-induced error. Finally, the part is moved to stage 3, where a locator has been deviated from its nominal position, which produces a deviation of part location and thus, the drill is misplaced producing a fixture-induced error. As it can be seen, in MMPs where machining operations are conducted, three main sources of errors arise: *Machining-induced errors*, *Datum-induced errors* and *Fixture-induced errors*. Note that a similar reasoning can be conducted in assembly lines where welding operations are performed instead of machining operations.

Despite being very common manufacturing systems in industry, the MMPs are usually too complex to be mathematically modeled and the development of tools and strategies for effective quality assurance and fault diagnosis is currently a challenging task that hinders the deployment of zero-defect manufacturing processes. In the literature, some approaches have been proposed to model the error propagation within these types of manufacturing systems. One of these approaches is the so-called Stream-of-Variation (SoV) approach, which was successfully developed in the late 90s for multi-stage assembly processes by Jin and Shi [2]. The SoV model is based on the State-Space Model from control theory to define mathematically the relationships between fixture and machining errors on machined surfaces, and the datum errors are introduced to link the errors between the stages. The SoV model was expanded to include multi-stage machining processes in [3] and later, the model was highly improved by Zhou et al. [4] with the introduction of Differential Motion Vectors (DMVs) to model the small displacements of each geometrical feature as it is used in the field of robotics [5]. This model can be considered as the SoV reference model within multi-stage machining processes, where the methodology to derive the model is explained in detail under the limitation of fixture devices based on 3-2-1 punctual locators. The model was expanded by Abellán-Nebot et al. [6] to include specific machining errors such as tool wear errors, deflection errors, kinematic errors from tool axis, and so on. In regards to assembly processes, the SoV model was firstly developed for rigid sheet metal parts in [2] but it was later extended to deal with compliant sheet metal parts by Camelio et al. [7]. In [8], the SoV model was expanded to deal with compliant parts using N-2-1 locating schemes based on punctual locators and later, the mathematical derivation to consider 3D rigid assemblies instead of sheet metal parts was presented in [9]. More recently the model was also extended to deal with composites in multi-stage assembly processes for the aeronautic industry considering compliant parts with anisotropic properties [10].

The application of the SoV model has been widely studied in the last two decades and promising results have been presented in different fields such as fault diagnosis and quality control [11]–[16], process planning [17], [18], manufacturing tolerance allocation and predictive maintenance [19], [20] and so on. However, despite the efforts made by many researchers, the SoV model still presents some drawbacks for its application in MMPs. One of the major criticisms refers to fixture error modeling, which is focused on punctual locators based on 3-2-1 schemes or N-2-1 schemes when compliant parts are considered, but positioning cases with plane/plane contact or cylinder/cylinder floating contact are not considered [21]. Under 3-2-1 schemes, the touching points between the locating surface and the fixture device are known, and the mathematical model that relates the error of each locator and the deviation of workpiece location can be determined. However, other common fixture devices such as vices or chucks do not follow this behavior, and the touching points of the locating surface and the fixture device may depend on previous errors. In this situation, the mathematical model between fixture errors and workpiece location errors cannot be determined in advance, and it will depend on the workpiece errors at the moment of clamping. This problem was tackled by Abellán-Nebot et al. [22], where a generic procedure for modeling fixtures based on surfaces instead of punctual locators was presented. Although the methodology deals with different configurations which depend on previous errors, the research does not deal with specific fixtures such as vices and omits other types of fixtures such as chucks. More recently, the inclusion of the bench vice errors into the SoV model has been introduced in [23]. However, the proposed methodology only showed the result for a specific vice without deriving a generic approach based on differential and homogeneous transformation matrices among fixture/workpiece features. Therefore, more general vices or alternative ones (i.e., rotatory or universal vices) cannot be modeled. Furthermore, the applicability of the methodology is limited since there is no clear use of common workholding specifications into the modeling approach, which prevents their use in industry.

This paper shows a methodology to model the effect of fixturing errors from two common fixtures in MMPs: 3-jaw chucks and bench vices. The mathematical development of these models follow the structure of the SoV model proposed in aforementioned studies, providing compatibility with the general SoV approach. The model includes different workholding configurations and it is also shown how to include the workholding accuracy to estimate part quality. The mathematical derivation of the models is validated through both CAD simulations and machining experimentation proving the high accuracy of the model despite linearization errors. Please, note that despite the low accuracy of these workholding devices in comparison with dedicated fixtures, their level of clamping and locating accuracy can be enough for low volume

production systems where manufacturing tolerances of tenths of a millimeter are allowed [24] and, thus, the inclusion of these devices into the SoV model may be of interest.

The paper is organized as follows. Section III provides the general methodology of the SoV model in order to identify the parts of the model that have to be extended. Section IV shows the mathematical derivation of the fixture- and datum-induced errors for bench vices, whereas Section V presents the mathematical derivation for 3-jaw chucks. Section VI shows a case study where a MMP with both types of fixtures is applied and the model is validated through CAD simulations and machining experiments. Finally, Section VII shows the conclusions of the paper.

III. Methodology Overview - The Stream of Variation model

The Stream-of-Variation (SoV) model uses the DMVs to define dimensional deviations of part features from nominal positions. As each feature is determined by a Local Coordinate System (LCS), DMVs define the displacement of each LCS from its nominal position (^{0}LCS). This displacement is composed of a position deviation vector $\mathbf{d}_L^{^0L} = [d_{Lx}^{^0L}, d_{Ly}^{^0L}, d_{Lz}^{^0L}]^T$ and an orientation deviation vector $\boldsymbol{\theta}_L^{^0L} = [\theta_{Lx}^{^0L}, \theta_{Ly}^{^0L}, \theta_{Lz}^{^0L}]^T$, so a DMV is defined as $\mathbf{x}_L^{^0L} = [(\mathbf{d}_L^{^0L})^T, (\boldsymbol{\theta}_L^{^0L})^T]^T$. In regards of nominal values, each ^{0}LCS is referred to the reference coordinate system (RCS) using a locating vector that defines its position $\mathbf{t}_{^0L}^R = [t_{^0Lx}^R, t_{^0Ly}^R, t_{^0Lz}^R]^T$ and its orientation $\boldsymbol{\omega}_{^0L}^R = [\omega_{^0Lx}^R, \omega_{^0Ly}^R, \omega_{^0Lz}^R]^T$. In this paper, terms $\omega_{^0Lx}^R, \omega_{^0Ly}^R$ and $\omega_{^0Lz}^R$ are expressed as proper Euler angles between RCS and ^{0}LCS in a Z-Y'-Z" order (this means a rotation of RCS around its Z axis, followed by a rotation around the new Y axis, and lastly, a rotation around the new Z axis). Fig. 2 shows an example of a locating vector of a machined feature and its corresponding DMV to model the deviation of the feature from nominal values.

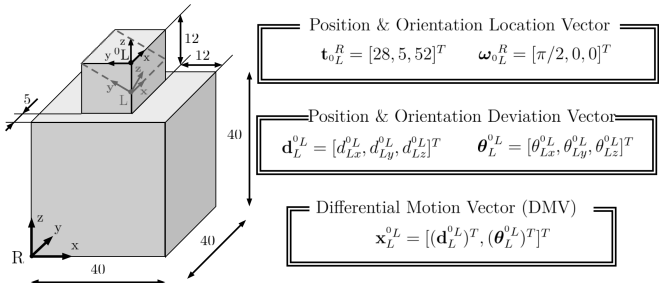

Fig. 2: Example of a DMV in a machining process.

In the SoV model, the deviations of all features are stacked up in a vector, denoted as $\mathbf{x}_k = [(\mathbf{x}_k^1)^T, (\mathbf{x}_k^2)^T, ..., (\mathbf{x}_k^M)^T]^T$, where $k = 1, ..., N$ refers to the number of the stage and $\mathbf{x}_k^1, ..., \mathbf{x}_k^M$ are the DMV of features $1, ..., M$. As it was pointed out above, the error propagation throughout the MMP is conducted by the adoption of the State-Space Model from control theory. Under this framework, the SoV model in a MMP of N-stages can be defined as [4]

$$\mathbf{x}_k = \mathbf{A}_{k-1} \cdot \mathbf{x}_{k-1} + \mathbf{B}_k^f \cdot \mathbf{u}_k^f + \mathbf{B}_k^m \cdot \mathbf{u}_k^m + \mathbf{w}_k, \qquad (1)$$

where $\mathbf{A}_{k-1} \cdot \mathbf{x}_{k-1}$ represents the variations transmitted by datum features generated at upstream stages, $\mathbf{B}_k^f \cdot \mathbf{u}_k^f$ represents the fixture-induced variations within stage k, where $\mathbf{u}_k^f$ denotes the fixture errors; $\mathbf{B}_k^m \cdot \mathbf{u}_k^m$ represents the machining-induced variations within stage k, where the cutting-tool path deviation is denoted as $\mathbf{u}_k^m$; and $\mathbf{w}_k$ is the un-modeled system noise and linearization errors. The derivation of this model is detailed in [4], where it is presented the procedure to obtain matrices $\mathbf{A}_{k-1}$, $\mathbf{B}_k^f$ and $\mathbf{B}_k^m$ at each stage, according to given product and process information (part geometry and fixture layouts). Fig. 3 shows the auxiliary matrices to build the SoV main matrices according to the methodology detailed in Zhou's et al. research work [4]. Following their methodology, the matrices $\mathbf{A}_{k-1}$, $\mathbf{B}_k^f$ and $\mathbf{B}_k^m$ are defined as

$$\mathbf{A}_{k-1} = [\mathbf{A}_k^1 + \mathbf{A}_k^5 \cdot \mathbf{A}_k^4 \cdot \mathbf{A}_k^2 \cdot \mathbf{A}_k^1], \qquad (2)$$

$$\mathbf{B}_k^f = [\mathbf{A}_k^5 \cdot \mathbf{A}_k^4 \cdot \mathbf{A}_k^3], \qquad (3)$$

$$\mathbf{B}_k^m = [\mathbf{A}_k^5], \qquad (4)$$

where $\mathbf{A}_k^1$ is the relocating matrix, $\mathbf{A}_k^2$ is the datum-induced variation matrix, $\mathbf{A}_k^3$ is the fixture-induced variation matrix, $\mathbf{A}_k^4$ is the feature generation matrix, and $\mathbf{A}_k^5$ is the selector matrix. Matrices $\mathbf{A}_k^2$ and $\mathbf{A}_k^3$ are currently derived for 3-2-1 punctual schemes [4], the N-2-1 extension [7], general punctual fixture configurations [8] and surface based fixtures [22].

The next sections presents the mathematical derivation of the corresponding matrices $\mathbf{A}_k^2$ and $\mathbf{A}_k^3$ when the workholding device is a bench vice or a 3-jaw chuck. Please note that in this paper it is assumed that the workpiece acts as a rigid part and errors due to deformation during clamping are assumed to be negligible in comparison with fixture- and datum-induced errors. For the sake of simplicity form errors are assumed to be negligible, but their inclusion can be straightforward when using small jaws or locators by treating form tolerances as an independent fixture error on each locator/jaw, as it is explained in [25]. If surfaces are used for locating, e.g. vice jaws, it can be considered that form errors have little or no effect on the result, as a feature's form tolerance is always smaller that its location/orientation tolerance. Form errors will be only significant if the surfaces in contact present an specific shape and the high points of both surfaces are aligned and touch each other, which is very remote [26, Chapter 20].

IV. Bench vices

Bench vices are common devices for holding workpieces on a milling machine table. Among bench vices, plain vices are probably the most widely used fixture device in shop-floor. A plain vice has two jaws, one fixed and one movable, and the workpiece is held by the force exerted from the movable jaw to the fixed one with a pull-down action. Although the jaws are usually plain, special jaws with irregular shape are sometimes used to hold non-prismatic parts. Figure 4a shows a typical bench vice for milling where the components of the vice (jaws, supports and pins) and the fixture coordinate system (FCS) are identified; Figure 4b shows the workpiece held in the vice and the datums CS: A-CS, B-CS and C-CS.

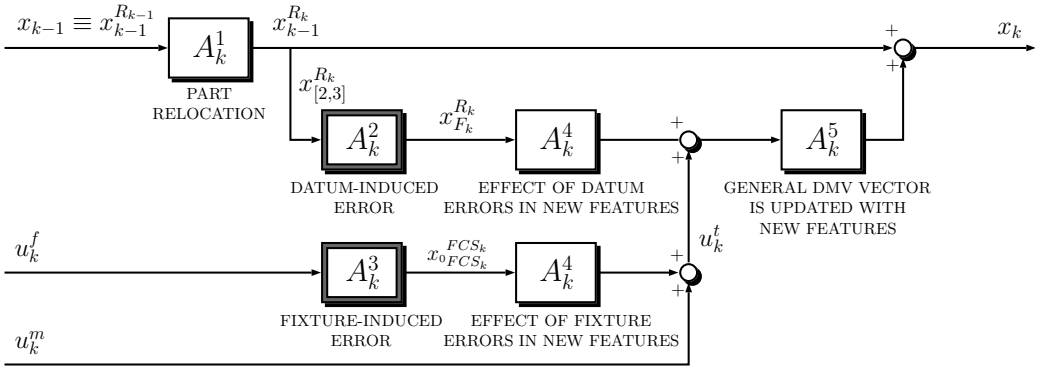

Fig. 3: Steps for modeling the Stream of Variation (SoV) of a MMP.

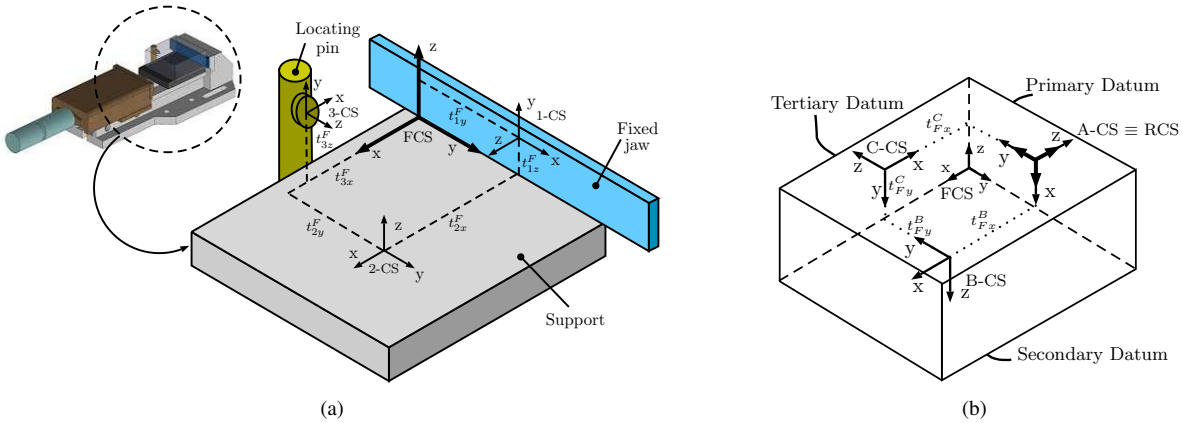

Fig. 4: a) Typical bench vice and definition of the FCS; b) workpiece held in the vice and datum coordinate systems.

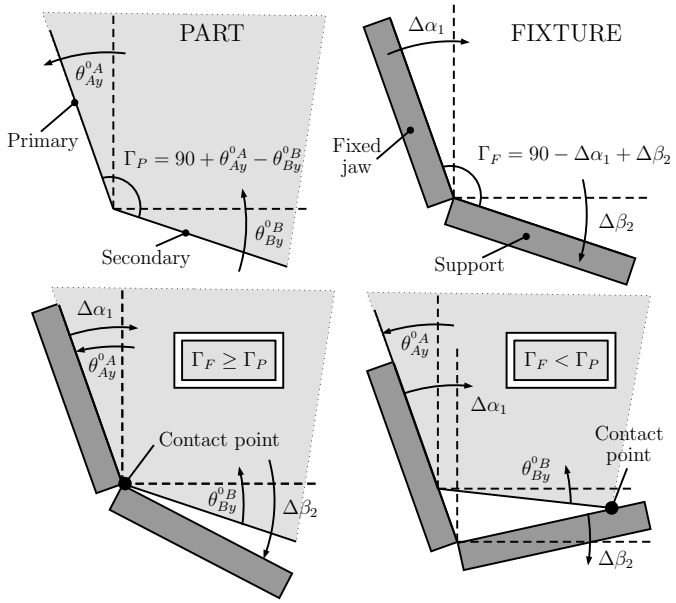

Fig. 5: Different part location due to different fixture and datum errors. The arrows indicate the positive direction of each angle.

Following the methodology proposed in [4], the relationship between the errors of vice surfaces (fixture-induced errors) and the deviation of the FCS is defined by the matrix $\mathbf{A}_k^3$, and the relationship between the errors of datum surfaces and the position of the FCS (datum-induced errors) is defined by matrix $\mathbf{A}_k^2$. However, it should be noted that the final assembly fixture-workpiece depends on the position and orientation deviation of the fixed jaw, the support surface and primary and secondary datums and thus, the superposition of fixture and datum errors as presented in previous researches cannot be straightforward applied. In other words, the values of both matrices $\mathbf{A}_k^2$ and $\mathbf{A}_k^3$ should be expressed as a function of the interaction between current position and orientation of datum and locating surfaces.

A. Fixture-induced errors

To understand the FCS deviation due to fixture errors, let us explain the clamping process in a plain vice. First, the workpiece is placed over the support which makes the support surface and primary datum to be coplanar. Then, the workpiece is moved over the support to touch first the primary datum with the fixed jaw and then, to touch the tertiary datum with the pin of the vice. Finally, the movable jaw moves until it clamps the part, exerting a force towards the fixed jaw and the support due to its pull-down action. Due to this clamping force, the primary datum will move to be coplanar with the fixed jaw which may cause that the

secondary datum lifts from the support. Therefore, the fixed jaw blocks three degrees of freedom (DOF), two rotations and one translation; the support blocks other two DOF, one rotation and one translation, and the pin blocks the remaining DOF.

The fixturing errors in vice fixtures can be defined as

$$\mathbf{u}_k^F = [\Delta z_1, \Delta\alpha_1, \Delta\beta_1, \Delta z_2, \Delta\alpha_2, \Delta\beta_2, \Delta z_3]^T, \quad (5)$$

where $\Delta z_1, \Delta\alpha_1, \Delta\beta_1$ refer to the Z-axis deviation and orientation deviations around X and Y axis of the fixed jaw (1-CS), respectively; $\Delta z_2, \Delta\alpha_2, \Delta\beta_2$ refer to similar deviations but from the support (2-CS); and Δz_3 refers to the deviation of the locating pin of the vice fixture (3-CS). Therefore, the resulting deviation of the FCS due to fixture errors is defined as

$$\mathbf{x}_{{}_0^F F} = \mathbf{A}_k^3 \cdot \mathbf{u}_k^F, \quad (6)$$

where matrix $\mathbf{A}_k^3$ can be estimated as follows.

As stated above, in a vice workholding system there is a plane to plane contact between the fixed jaw and the primary datum. Thus, 3 DOF are blocked by the fixed jaw and the errors Δz_1, $\Delta\alpha_1$, and $\Delta\beta_1$ are directly propagated to the FCS in these DOF. Therefore

$$\delta\mathbf{H}_F^{{}_0^F} =^0 \mathbf{H}_1^F \cdot \mathbf{H}_1^{{}_0^1} \cdot \mathbf{H}_F^1, \quad (7)$$

where

$$\delta\mathbf{H}_F^{{}_0^F} = \begin{bmatrix} 1 & -\theta_{Fz}^F & \theta_{Fy}^F & d_{Fx}^F \\ \theta_{Fz}^F & 1 & \theta_{Fx}^F & d_{Fy}^F \\ -\theta_{Fy}^F & \theta_{Fx}^F & 1 & d_{Fz}^F \\ 0 & 0 & 0 & 1 \end{bmatrix} = \mathbf{I}_{4\times4} + \boldsymbol{\Delta}_F^{{}_0^F}, \quad (8)$$

and

$$\boldsymbol{\Delta}_F^{{}_0^F} = \begin{bmatrix} \hat{\boldsymbol{\theta}}_F^{{}_0^F} & \boldsymbol{d}_F^{{}_0^F} \\ \mathbf{0} & 0 \end{bmatrix}. \quad (9)$$

In Eq. (7), the HTM $\mathbf{H}_F^1$ is equal to ${}^0\mathbf{H}_F^1$ since there is a plane to plane contact and the movements along X axis and rotations around Y and Z axis of FCS are blocked. Then, considering $\delta\mathbf{H}_{{}_0^F F}^F = (\delta\mathbf{H}_F^{{}_0^F})^{-1} = \mathbf{I}_{4\times4} - \boldsymbol{\Delta}_F^{{}_0^F}$ and $\mathbf{x}_{{}_0^F F} = [d_{Fx}^F, d_{Fy}^F, d_{Fz}^F, \theta_{Fx}^F, \theta_{Fy}^F, \theta_{Fz}^F]^T$, Eq. (7) is solved to obtain the values of $\mathbf{x}_{{}_0^F F}(1)$, $\mathbf{x}_{{}_0^F F}(5)$ and $\mathbf{x}_{{}_0^F F}(6)$ as a function of Δz_1, $\Delta\alpha_1$, and $\Delta\beta_1$.

The secondary datum blocks other two DOF, the movement of the part along the Z axis of FCS and the rotation of the part around the X axis of FCS. Furthermore, since the plane to plane contact is given at the primary datum, the secondary datum and the support touch each other at least in two points. Denoting the two contact points as $\mathbf{p}_D$ and $\mathbf{p}_E$, where $\tilde{\mathbf{p}} = [\mathbf{p}^T, 1]^T$, we have

$$\begin{aligned} \tilde{\mathbf{p}}_D^F &= \mathbf{H}_{{}_0^F 1}^F \cdot \mathbf{H}_2^{{}_0^1} \cdot \tilde{\mathbf{p}}_D^2 \\ &= \delta\mathbf{H}_{{}_0^F F}^F \cdot \mathbf{H}_{{}_0^F 1}^{{}_0^F} \cdot \mathbf{H}_{{}_0^1 2}^{{}_0^1} \cdot \mathbf{H}_2^{{}_0^2} \cdot \tilde{\mathbf{p}}_D^2, \end{aligned} \quad (10)$$

and the same expression for $\tilde{\mathbf{p}}_E^F$ holds. From Eq. (10) we know that $\tilde{\mathbf{p}}_D^F(3) = \tilde{\mathbf{p}}_E^F(3) = 0$ since the contact points define the location of the part in Z direction of the FCS, and the orientation deviation along X axis is the same as the orientation deviation of the support which blocks this DOF. Thus, Eq. (10) can be solved to relate $\mathbf{x}_{{}_0^F F}(3)$ and $\mathbf{x}_{{}_0^F F}(4)$ with the fixed jaw errors together with the support errors.

Finally, the locating pin blocks the movement of the part along the Y axis, thus, following the same procedure we have

$$\begin{aligned} \tilde{\mathbf{p}}_G^F &= \mathbf{H}_{{}_0^1}^F \cdot \mathbf{H}_3^{{}_0^1} \cdot \tilde{\mathbf{p}}_G^3 \\ &= \delta\mathbf{H}_{{}_0^F F}^F \cdot \mathbf{H}_{{}_0^1 1}^{{}_0^F} \cdot \mathbf{H}_{{}_0^1 3}^{{}_0^1} \cdot \mathbf{H}_3^{{}_0^3} \cdot \tilde{\mathbf{p}}_G^3, \end{aligned} \quad (11)$$

where $\tilde{\mathbf{p}}_G$ is the contact point defined by the locating pin of the fixture and $\tilde{\mathbf{p}}_G^F(2) = 0$. Eq. (11) can be solved to relate $\mathbf{x}_{{}_0^F F}^F(2)$ with the locating pin errors together with support and fixed jaw errors.

Following the steps shown above, the DMV $\mathbf{x}_{{}_0^F F}^F$ can be expressed as a function of fixture errors through matrix $\mathbf{A}_k^3$. For the workpiece and vice shown in Figure 4 the numerical solution of this matrix is:

$$\mathbf{A}_k^3 = \begin{bmatrix} -1 & t_{1z}^F & -t_{1y}^F & 0 & 0 & 0 & 0 \\ 0 & 0 & t_{3x}^F & 0 & -t_{3z}^F & 0 & -1 \\ 0 & -a & 0 & -1 & t_{2y}^F & a - t_{2x}^F & 0 \\ 0 & 0 & 0 & 0 & -1 & 0 & 0 \\ 0 & -1 & 0 & 0 & 0 & 0 & 0 \\ 0 & 0 & -1 & 0 & 0 & 0 & 0 \end{bmatrix}, \quad (12)$$

where t_{1y}^F and t_{1z}^F refer to the location of the fixed jaw CS w.r.t. the FCS, t_{2x}^F and t_{2y}^F refers to the location of the support CS w.r.t. the FCS, and t_{3x}^F, t_{3z}^F refer to the location of the locating pin CS w.r.t. the FCS. Parameter a depends on the fixture and datum assembly and resulting contact points $\mathbf{p}_D$ and $\mathbf{p}_E$. As it is shown in Fig. 5, the contact points between part and fixture depend on orientation deviations of support and fixed jaw and orientation deviation of primary and secondary datums. For the example given in Fig 4, a has the following values:

$$a = \begin{cases} 0, & \text{if } \Gamma_F \geq \Gamma_P \\ L_s, & \text{otherwise} \end{cases}, \quad (13)$$

where L_s is the length of the contact between support and workpiece, $\Gamma_F = 90° + \Delta\beta_1 - \Delta\alpha_2$ and $\Gamma_P = 90° - \theta_{Ay}^{{}^0A} - \theta_{Bx}^{{}^0B}$.

For practical purposes, it is of interest to relate the fixture errors with the technical specifications of the vice. From common technical specifications, we may remark accuracy in clamping repeatability and parallelism and perpendicularity specification of vice surfaces. These geometrical specifications can be translated to DMV limits in the $\mathbf{u}_k^F$ parameters as shown in [25], and thus, the estimation of part quality variability for a given bench vice can be conducted. Therefore, considering L_v and H_v as the length and height of the fixed jaw, respectively; W_s as the contact width between support and part; and ϵ_c, ϵ_{pa} and ϵ_{pe} as clamping accuracy and parallelism and perpendicularity of vice surfaces, we have: $|\Delta\alpha_2| \leq \epsilon_{pa}/W_s$;

$|\Delta\beta_2| \leq \epsilon_{pa}/L_s$; $|\Delta z_1| \leq \epsilon_c/2$; $|\Delta\alpha_1| \leq \epsilon_{pe}/H_v$; $|\Delta\beta_1| \leq \epsilon_{pe}/L_v$; and their relationships are defined as:

$$L_v \cdot |\Delta\beta_1| + H_v \cdot |\Delta\alpha_1| \leq \epsilon_{pe}. \tag{14}$$

$$L_s \cdot |\Delta\beta_2| + W_s \cdot |\Delta\alpha_2| \leq \epsilon_{pa}, \tag{15}$$

Additionally, we may add the alignment error of the vice in the machine-tool as ϵ_{alig} and the position error of the vice on the machine-tool table during the setup process (e.g., touch probe inaccuracy) as ϵ_{stp}. Therefore, we have $|\Delta z_2| \leq \epsilon_{stp}$, $|\Delta z_1| \leq \epsilon_c/2 + \epsilon_{stp}$ and $\Delta\beta_1$ previously defined will add the alignment error ϵ_{alig}.

Another common vice configuration is presented when the location of the workpiece in the parallel direction of the jaws is undefined so the pin locator is removed from the workholding device. Under this configuration, the possible deviation of machined features along this direction is undetermined, and t^F_{3x} and t^F_{3z} from matrices $\mathbf{A}^2_k$ and $\mathbf{A}^3_k$ are replaced by U which refers to an undetermined component. To operate with U, the following properties apply:

$$\forall b \in \mathbb{R}, b + U = U; \forall b \in \mathbb{R}, b \cdot U = U. \tag{16}$$

B. Datum-induced errors

Considering the primary datum as the reference coordinate system (RCS) of the workpiece, the deviation of the FCS w.r.t. RCS is modeled by the DMV $\mathbf{x}^R_F$ and it can be defined as [4]

$$\mathbf{x}^R_F = \mathbf{T}_1 \cdot \mathbf{x}^R_2 + \mathbf{T}_2 \cdot \mathbf{x}^R_3 = \mathbf{A}^2_k \cdot \left[\mathbf{x}^R_2 \ \mathbf{x}^R_3\right]^T, \tag{17}$$

where $\mathbf{x}^R_2$ and $\mathbf{x}^R_3$ are the DMV that define the deviations of the secondary and tertiary datums of the workpiece which correspond with the workpiece surfaces that touches the support and the locating pin, and $\mathbf{A}^2_k = [\mathbf{T}_1 \ \mathbf{T}_2]$. Following the procedure presented in [4], [23], the matrices $\mathbf{T}_1$ and $\mathbf{T}_2$ for the vice and workpiece shown in Fig. 4 are defined as

$$\mathbf{T}_1 = \begin{bmatrix} 0 & 0 & 0 & 0 & 0 & 0 \\ 0 & 0 & 0 & -t^F_{3z} & 0 & 0 \\ 0 & 0 & -1 & -t^B_{Fy} & (a - t^B_{Fx}) & 0 \\ 0 & 0 & 0 & 1 & 0 & 0 \\ & & & \mathbf{0}_{2\times 6} & & \end{bmatrix}, \tag{18}$$

$$\mathbf{T}_2 = \begin{bmatrix} 0 & 0 & 0 & 0 & 0 & 0 \\ 0 & 0 & -1 & (t^F_{3z} - t^C_{Fy}) & (t^C_{Fx} - t^F_{3x}) & 0 \\ & & & \mathbf{0}_{4\times 6} & & \end{bmatrix}, \tag{19}$$

where t^B_{Fx} and t^B_{Fy} are the X and Y coordinate of FCS w.r.t. B-CS, respectively, t^C_{Fx} and t^C_{Fy} are the same but w.r.t. the C-CS, t^F_{3x} and t^F_{3z} refers to the position of the locating pin of the vice and the parameter a depends on fixture and workpiece assembly (Fig. 5) and presents the values shown in Eq. (13). Please, refer to Appendix A for the derivation details of $\mathbf{T}_1$ and $\mathbf{T}_2$.

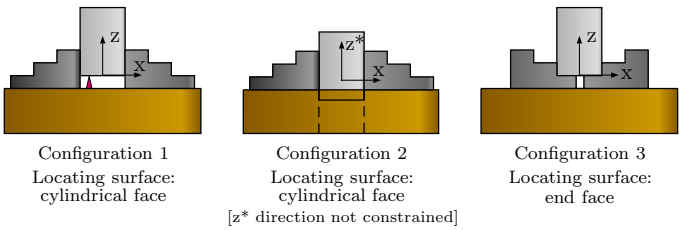

Fig. 6: Typical configurations of a 3-jaw self-centering chuck and definition of the FCS.

V. 3-JAW SELF-CENTERING CHUCKS

A 3-jaw self-centering chuck is a workholding device used in turning and milling processes to hold regular-shaped parts such as cylinders. This type of chuck consists of a cylindrical base with three slots carved from the center to the exterior, separated 120° from each other. There is a jaw in each slot, and all three jaws slide simultaneously by the same amount if one of the three pinions is rotated. A 3-jaw chuck can present different configurations depending on the main locating surfaces used. Figure 6 shows three configurations analyzed in this paper. In the first configuration, the main locating surface is the outer diameter of the workpiece and thus, the jaws block 4 DOF whereas a pin locator blocks the Z movement of the part. The second configuration is similar to the previous one but no locating pin is used, so the position of the workpiece in Z direction is undetermined. The third configuration uses the end flat surface of the workpiece as the main locating surface which blocks 3 DOF (the Z movement and two rotations) due to the contact with the jaws. In this configuration, the clamping process locates the part in X and Y direction. In all cases, rotation around the Z-axis is limited by the friction of the workpiece and the jaws.

A. Fixture-induced errors

Some researches have studied the errors of 3-jaw chucks and the methods to improve chuck accuracy [24], [27], [28]. The main identified errors in 3-jaw chucks are: radial displacement error of individual jaws due to internal wear or backlash; taper in jaw alignment; non-symmetric deformation of jaw-workpiece and kinematic redundancy. In this paper, we consider that the results of those fixture errors are reflected in the deviation of the jaws from their nominal position and orientation. Therefore, we consider as fixture errors the position deviation of each jaw in the radial direction, the position error of the locating pin or the jaw to place the end face of the workpiece, and the orientation error due to jaw alignment.

For any of the chuck configurations defined above, the position of the workpiece in X and Y axis is defined by the position deviation of each jaw in the radial direction. Considering that the jaws are placed perpendicular to the slots and the chuck base, the top-down view of a chuck holding a perfect cylinder (XY view) can be defined as in Figure

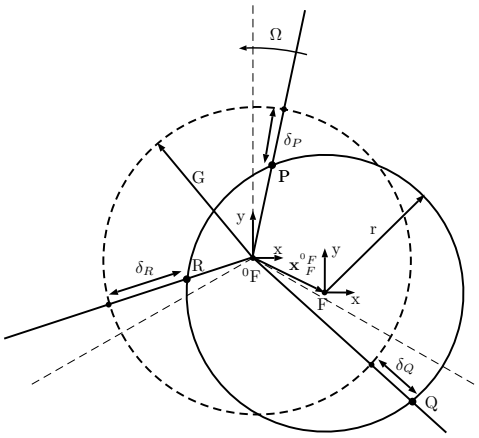

Fig. 7: Deviation of FCS due to self-centering errors. Errors are exaggerated for illustrative purposes.

7. Points P, Q and R (the contact point of the jaws) are separated a distance G from the center plus a jaw error δ, expressed outwards the center. Thus, the deviation of the jaws from nominal positions are denoted as δ_P, δ_Q and δ_R. The deviation of the center of the workpiece clamped with respect to the center of the chuck is estimated to be $2/3$ of the jaw deviation along the direction of jaw deviation, as it is shown in the Appendix B.

Furthermore, the workpiece may be deviated from the Z axis if the chuck constrains this direction as in configuration 1 and 3. In configuration 1, the main locating surface is the cylindrical surface of the workpiece and an orientation deviation of the jaws will produce a Z deviation of the part when the end face and the locating pin of the chuck touch each other. In configuration 3, the main locating surface is the end face of the workpiece, and the Z deviation will depend on the position and orientation deviation of the plane defined by the 3 jaws that contact with the end face. In any case, we represent the Z deviation as δ_z, and the orientation deviation of the chuck as δ_α and δ_β, which reproduces the same inclination of the FCS from its nominal position.

Therefore, the fixture errors in a 3-jaw chuck can be defined as

$$\mathbf{u}_k^F = [\delta_P \ \delta_Q \ \delta_R \ \delta_z \ \delta_\alpha \ \delta_\beta]^T, \tag{20}$$

and the corresponding matrix $\mathbf{A}_k^3$ can be defined as $[\mathbf{A}_{k(1)}^3 \ \mathbf{A}_{k(2)}^3]^T$, where

$$\mathbf{A}_{k(1)}^3 = \begin{bmatrix} \frac{2}{3}\sin\Omega & -\frac{2}{3}\cos\Omega \\ -\frac{\sqrt{3}}{3}\cos\Omega - \frac{1}{3}\sin\Omega & -\frac{\sqrt{3}}{3}\sin\Omega + \frac{1}{3}\cos\Omega \\ \frac{\sqrt{3}}{3}\cos\Omega - \frac{1}{3}\sin\Omega & \frac{\sqrt{3}}{3}\sin\Omega + \frac{1}{3}\cos\Omega \\ \mathbf{0}_{3\times 2} \end{bmatrix}, \tag{21}$$

$$\mathbf{A}_{k(2)}^3 = \begin{bmatrix} \mathbf{0}_{3\times 3} & \mathbf{0}_{3\times 1} \\ -\mathbf{I}_{3\times 3} & \mathbf{0}_{3\times 1} \end{bmatrix}. \tag{22}$$

Please, note that if the configuration 2 applies, there is no control about the Z position of the workpiece and thus, Δz_L is replaced by U, an undetermined component. From previous equations, the angle Ω has been included to take into account that the position of the jaws may be rotated from the FCS on the machine-tool table so jaw P may be not in the $+Y$ direction. Furthermore, note that if $\delta_P = \delta_Q = \delta_R$ then the center of the part is the same as the center of the chuck and thus, $\mathbf{x}_F^{^0F}(1) = \mathbf{x}_F^{^0F}(2) = \mathbf{0}$.

As it was presented in the vice, it is of interest to obtain the relation between the technical specifications about accuracy of the 3-jaw chuck and the identified fixture errors. Common technical specifications in chucks refer to maximum TIR (total indicator runout) values in radial and axial direction, as it is shown in Figure 8. As it has been shown, the deviation of the jaws will define the centering error which in turn produces a constant radial run-out defect when rotating a cylindrical part. For the configuration 3 (Fig 8a), the radial TIR alongside the jaws, denoted as TIR^r, can be defined as two times the centering offset and thus, this accuracy term of the chuck can be represented as the deviation of the jaws, δ_P, δ_Q and δ_R, in a range of $[0, \frac{3}{4}\cdot TIR^r]$. On the other hand, the axial TIR is related to the orientation deviation of the chuck defined by δ_α and δ_β and the diameter of the tested part. Denoting TIR^a as the axial TIR and D_t the diameter of the part tested for the axial TIR, we have $|\delta_\alpha| \leq TIR^a/D_t$ and $|\delta_\beta| \leq TIR^a/D_t$, and the following relationship holds:

$$D_t \cdot \sqrt{\delta_\alpha^2 + \delta_\beta^2} \leq TIR^a. \tag{23}$$

For the configuration 1 (Fig 8b), the radial TIR is measured at the length L_t of the tested part. Similar to the configuration 3, the deviation of jaws are limited to a range of $[0, \frac{3}{4}\cdot TIR^r]$ but now, due to the effect of orientation deviations δ_α and δ_β at the L_t position of the dial indicator, we have $|\delta_\alpha| \leq TIR^r/(2L_t)$ and $|\delta_\beta| \leq TIR^r/(2L_t)$, and additionally, the following relationship holds:

$$4/3 \cdot \sqrt{(\delta_P - 0.5(\delta_Q + \delta_R))^2 + (c^* \cdot (\delta_Q - \delta_R))^2} + L_t \cdot \sqrt{\delta_\alpha^2 + \delta_\beta^2} \leq TIR^r, \tag{24}$$

where $c^* = cos(30°)$.

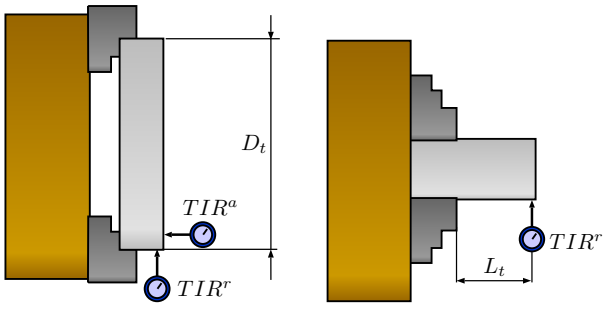

(a) (b)

Fig. 8: Common radial and end face (axial) runout used for test certifications in 3-jaw chucks with a) configuration 3, b) configuration 1 and 2.

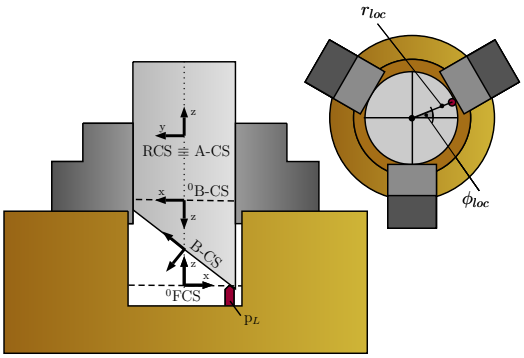

Fig. 9: Effect of datum errors on part location.

B. Datum-induced errors

Datum-induced errors in 3-jaw chuck mainly depend on the chuck configuration. A chuck with configuration 2 presents only a primary datum, the cylindrical feature, and there is no secondary datum since there is no constraint over the Z position of the workpiece. Therefore, no datum-induced errors apply. Similarly, a chuck with configuration 3 presents the end face of the workpiece as the primary datum and the cylindrical feature is defined as the secondary datum. Since the chuck is a self-centering chuck and form errors are not considered, the center of the workpiece would be only defined by the jaw errors even though the cylindrical feature would present a orientation deviation, so no datum-induced errors apply. However, when the chuck presents the configuration 1, where a locating pin block the Z movement of the part and the primary datum is the cylindrical feature, a datum-induced error may arise as shown in Fig. 9. As it can be seen, only the position along nominal Z-axis is modified due to datum errors since the cylindrical surface is oriented according to the 3-jaw orientation which is considered perfect when only datum-induced errors are analyzed. Then, following the methodology presented in [4], the deviation of the nominal FCS w.r.t. RCS, $\mathbf{x}_F^R$, can be obtained as

$$\mathbf{x}_F^R = \mathbf{T}_1 \cdot \mathbf{x}_2^R = \mathbf{A}_2 \cdot \mathbf{x}_2^R, \tag{25}$$

where $\mathbf{x}_2^R$ is the deviation of the secondary datum w.r.t. the part reference CS. The solving steps are detailed in Appendix C. Once solved, the deviation of the FCS w.r.t. RCS in Z axis direction is defined as

$$\mathbf{x}_F^R(3) = -d_{Bz}^R - p_{Ly}^F \cdot \theta_{Bx}^R - p_{Lx}^F \cdot \theta_{By}^R, \tag{26}$$

In matrix form, the final matrix $\mathbf{A}_k^2$ from Zhou's methodology can be expressed as

$$\mathbf{A}_k^2 = \begin{bmatrix} 0 & 0 & 0 & 0 & 0 & 0 \\ 0 & 0 & 0 & 0 & 0 & 0 \\ 0 & 0 & -1 & -p_{Ly}^F & -p_{Lx}^F & 0 \\ 0 & 0 & 0 & 0 & 0 & 0 \\ 0 & 0 & 0 & 0 & 0 & 0 \\ 0 & 0 & 0 & 0 & 0 & 0 \end{bmatrix}. \tag{27}$$

Note that $\mathbf{p}_L^F$ is the position of the locating point w.r.t. FCS and it depends on the distance from the center of the chuck, r_{loc}, and the angle w.r.t. the X axis of FCS, ϕ_{loc}, as it is shown in Fig. 9. Then, the X and Y coordinate w.r.t. FCS are

$$p_{Lx}^F = r_{loc} \cdot \cos(\phi_{loc}); \tag{28}$$
$$p_{Ly}^F = r_{loc} \cdot \sin(\phi_{loc}). \tag{29}$$

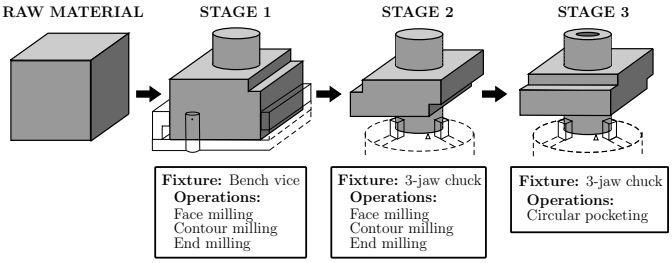

Fig. 10: 3-stage machining process evaluated.

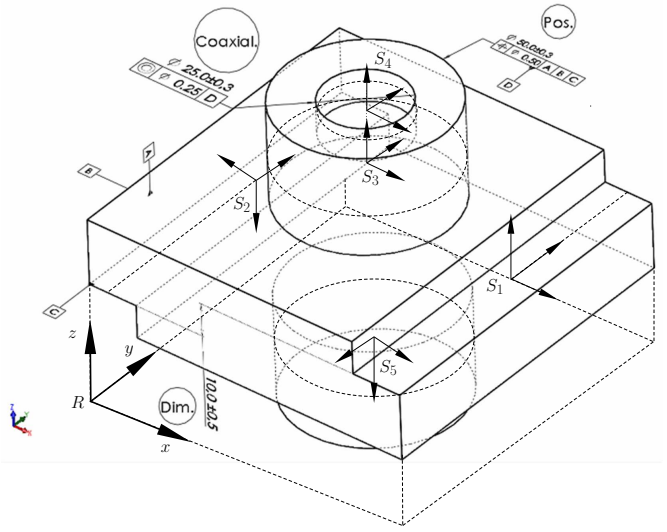

Fig. 11: Part specifications to be inspected. Other dimensions are omitted for simplicity.

VI. Case Study

In order to validate the extension of the SoV model, a 3-stage machining process is analyzed where both bench vices and 3-jaw chucks are used. As it is shown in Fig. 10, the manufacturing process consists of a face milling and end-milling operation at the first stage holding the part on a bench vice, a second stage where similar machining operations are conducted but using as fixturing device a 3-jaw chuck with a centered locator, and a third stage where the part is held on the same 3-jaw chuck in order to conduct a circular pocketing operation. As shown in Fig. 11, the inspected part specifications are: distance between both square-shoulder features, position of cylinder with respect to datums A, B, C, and the coaxiality of the circular pocketing with respect to its datum D. The position and orientation vectors for the main features are shown in Table I. The raw material is an aluminum block with dimensions 100 x 100 x 100 mm whose surfaces have been premachined so flatness and square errors between surfaces can be assumed negligible.

TABLE I: Position and orientation vectors of main feature CS.

Feature	$\mathbf{t}^R$	$\boldsymbol{\omega}^R$
S_1	$[92.5, 50, 55]^T$	$[0, 0, 0]^T$
S_2	$[7.5, 50, 45]^T$	$[0, \pi, 0]^T$
S_3	$[50, 50, 80]^T$	$[0, 0, 0]^T$
S_4	$[50, 50, 90]^T$	$[0, 0, 0]^T$
S_5	$[50, 50, 20]^T$	$[\pi, \pi, 0]^T$

Fig. 12: Machining center, workholding devices and machined part from case study.

The validation is conducted in two ways: 1) by using the SoV model to predict the deviations of the 3 geometrical specifications of the part and comparing these results with the resulting deviations obtained using a CAD software and; 2) by machining the part and comparing the results with those expected by the SoV and CAD model. The CAD software used is SolidWorks, and we basically model the fixture-workpiece assembly with the surface errors introduced in the tested cases to check the final part deviation. This is a tedious and time-consuming procedure that can be used for checking the effect of few errors at the same time assuming the rest negligible, and it cannot be used for checking the manufacturing process capability. For the machining experimentation, the machining center used for the experimentation is a Deckel Maho DMC 70V machining center, and the features are inspected in a Brown & Sharpe Mistral 775 coordinate measuring machine. The vice used is a Fresmak Arnold Twin with 0.02 mm of parallelism and perpendicularity and 0.01 mm clamping accuracy, and the 3-jaw chuck is a Optimum K11-125 chuck model mounted according to configuration 1 with an inspected TIR^r of 0.11 mm for a length of $L_t = 50$ mm. The setup process of the vice and 3-jaw chuck in the machine-tool table is conducted with a Renishaw touch probe and the alignment and positioning error is assumed to be $\epsilon_{alig} = 0.020$ mm/100 mm and $\epsilon_{stp} = \pm 0.015$ mm. A first part is machined to calibrate the process (e.g., tool dimensions, offsets due to clamping deformation, etc.). Figure 12 illustrates the experimental setup.

Three different situations are tested: i) no errors; ii) relative small fixture errors; and iii) severe fixture errors. The fixture errors that were intentionally added, cases ii) and iii), are shown in Table II. These errors were physically introduced by

TABLE II: Errors added in the multi-stage machining process. Ω is 0 in stages 2 and 3.

Case	Stage 1 (Vice errors)	Stage 2 (Chuck errors)	Stage 3 (Chuck errors)
i	no errors added	no errors added	no errors added
ii	$\Delta z_1, \Delta z_2 = 0.1\ mm$ $\Delta z_3 = 0.1\ mm$	$\delta_P = 0.2\ mm$ $\delta_z = 0.1\ mm$	$\delta_P = 0.2\ mm$ $\delta_z = 0.1\ mm$
iii	$\Delta\alpha_1 = -0.01\ rad$ $\Delta z_2, \Delta z_3 = 0.3\ mm$ $\Delta z_1 = 0.35\ mm$	$\delta_P = 0.5\ mm$ $\delta_z = 0.3\ mm$	$\delta_P = 0.5\ mm$ $\delta_z = 0.3\ mm$

adding a feeler gauge between the workholding device and the workpiece or modifying the zero part coordinate system in the CNC maching-tool to get the same effect. Furthermore, the SoV model is applied in two ways. The first one considers the errors added into the process and assumes negligible any other errors. Conversely, the second one, named as "SoV + Monte Carlo", considers the technical specifications related to the accuracy of the workholding systems and simulates additional errors according to these specifications in order to calculate a range of values for each inspected specification. For this purpose, 5,000 Monte Carlo simulations were run and the range that comprises the 99.7% of the values was recorded.

The results are shown in Table III. Firstly, the case i) shows the estimation of the range of values for the analyzed part specifications considering the accuracy technical specifications of the vice and the 3-jaw chuck used. These ranges are in fact the manufacturing process capability according to the workholding specifications and assuming no machining-induced errors exist. For this case study, the high TIR of the 3-jaw chuck used is reflected on the high expected coaxility error which is indeed confirmed in the experimentation. However, the specification related to the position error of the cylinder can be kept tight despite the bench vice inaccuracies, ensuring a position error less than 0.029 mm under Monte Carlo simulations and experimentally validated with a measured error of 0.035 mm. Secondly, for both small and severe errors added into the process, the proposed model shows a maximum error of 1% in comparison with the CAD results. The first specification (dimensional deviation between square-shoulder features), gives the same results between CAD and SoV model because, given the errors in Table II, only the deviation in Z direction of the 3-jaw chuck at stage 2 has an impact and then, there is no error due to linearizations. However, the position specification shows the effect of linearization errors in the vice due to orientation deviations when comparing with respect to CAD results. According to the results, this error is around 1%.

Finally, the results from the SoV model considering the errors added and the accuracy specifications of the workholding systems are compared with the results obtained after machining and inspecting the parts. As it is shown in Table III, the inspected specifications are in good agreement with the estimated range of values. The position specifications present a slightly higher values than the ones

TABLE III: Validation results. Comparison between SoV model, CAD simulations and machined parts. Units in mm.

	CAD			SoV			SoV + Monte Carlo			Experimental (Machined parts)		
#	Dim.	Pos.	Coaxial.	Dim.	Pos.	Coaxial.	Dim.	Pos.	Coaxial.	Dim.	Pos.	Coaxial.
i	10.000	0.000	0.000	10.000	0.000	0.000	$[9.974, 10.026]$	$[0, 0.029]$	$[0, 0.225]$	9.986	0.035	0.109
ii	9.900	0.141	0.188	9.900	0.141	0.188	$[9.875, 9.927]$	$[0.121, 0.164]$	$[0.040, 0.404]$	9.868	0.154	0.358
iii	9.700	0.392	0.471	9.700	0.390	0.471	$[9.675, 9.726]$	$[0.370, 0.410]$	$[0.312, 0.687]$	9.644	0.451	0.362

estimated through Monte Carlo which may be explained by machining-induced errors or deformation variations in the bench vice during clamping.

VII. Conclusions

This paper has shown how to extend the current SoV model in order to include general purpose workholding devices such as bench vices and 3-jaw chucks, not considered yet in the literature. In bench vices, the errors included in the model are position and orientation errors of plain jaws, supports and pins. In 3-jaw chucks, the errors included are the position error of jaws in the chuck, the position error of the locating pin to block the Z direction of the workpiece and the orientation errors of the jaws. In all cases, the model assumes that the workpiece acts as a rigid part and errors due to deformation during clamping are assumed to be negligible in comparison with fixture- and datum-induced errors. The model has been validated on a 3-stage machining process through both CAD simulations and machining experimentation. The model performance with respect to CAD simulations showed an error of less than 1% due to linearization and the machining results validated the capability of the model to estimate 99.7% confidence intervals for different product specifications considering the accuracy of the workholding systems. Unlike previous extensions of the model, the proposed extension let practitioners apply zero-defect strategies in multi-stage machining processes where bench vices or chucks are used and it can also be used for estimating manufacturing process capability under specific workholding devices.

Acknowledgements

This work was supported by the grant ACIF/2018/245 from Generalitat Valenciana (Spain).

Appendix A
Calculus of datum-induced errors in vices

Following the procedure explained in [4], we define the datum points that touch the secondary datum, denoted as $\mathbf{p_D}$ and $\mathbf{p_E}$, which depends on the relationship between the orientation errors of fixture surfaces 1 and 2 and datum surfaces A and B, and the datum point that touches the locating pin of the vice, $\mathbf{p_G}$. The nominal coordinates of these three points in FCS are denoted as $\mathbf{p_D^F}$, $\mathbf{p_E^F}$, and $\mathbf{p_G^F}$. Thus, we have

$$\mathbf{H}_R^B \cdot \mathbf{H}_F^R \cdot \tilde{\mathbf{p}}_D^F = \tilde{\mathbf{p}}_D^B, \tag{30}$$
$$\mathbf{H}_R^B \cdot \mathbf{H}_F^R \cdot \tilde{\mathbf{p}}_E^F = \tilde{\mathbf{p}}_E^B, \tag{31}$$
$$\mathbf{H}_R^C \cdot \mathbf{H}_F^R \cdot \tilde{\mathbf{p}}_G^F = \tilde{\mathbf{p}}_G^C. \tag{32}$$

Since the contact points between datums and fixture surfaces have a coordinate of 0 in Z axis w.r.t. the each datum coordinate system (note that all datum CS have a Z-axis pointing out to the surface), the coordinate Z of points $\mathbf{p_D^B}$, $\mathbf{p_E^B}$ and $\mathbf{p_G^C}$ are equal to 0. Following the steps in [4], previous equations can be simplified to the following expressions

$$\begin{bmatrix} [{}^0\mathbf{a}_B^F]^T & [\mathbf{p}_D^F \times {}^0\mathbf{a}_B^F]^T \\ [{}^0\mathbf{a}_B^F]^T & [\mathbf{p}_E^F \times {}^0\mathbf{a}_B^F]^T \\ [{}^0\mathbf{a}_C^F]^T & [\mathbf{p}_G^F \times {}^0\mathbf{a}_C^F]^T \end{bmatrix} \cdot \mathbf{x}_F^R = \begin{bmatrix} [[\boldsymbol{\theta}_B^R \times {}^0\mathbf{n}_F^B]_{(3)} & [\boldsymbol{\theta}_B^R \times {}^0\mathbf{o}_F^B]_{(3)} & [\boldsymbol{\theta}_B^R \times {}^0\mathbf{a}_F^B]_{(3)} & \boldsymbol{\theta}_B^R \times {}^0\mathbf{t}_F^B + \mathbf{d}_B^R]_{(3)}] \cdot \tilde{\mathbf{p}}_D^F \\ [\boldsymbol{\theta}_B^R \times {}^0\mathbf{n}_F^B]_{(3)} & [\boldsymbol{\theta}_B^R \times {}^0\mathbf{o}_F^B]_{(3)} & [\boldsymbol{\theta}_B^R \times {}^0\mathbf{a}_F^B]_{(3)} & \boldsymbol{\theta}_B^R \times {}^0\mathbf{t}_F^B + \mathbf{d}_B^R]_{(3)}] \cdot \tilde{\mathbf{p}}_E^F \\ [\boldsymbol{\theta}_C^R \times {}^0\mathbf{n}_F^C]_{(3)} & [\boldsymbol{\theta}_C^R \times {}^0\mathbf{o}_F^C]_{(3)} & [\boldsymbol{\theta}_C^R \times {}^0\mathbf{a}_F^C]_{(3)} & \boldsymbol{\theta}_C^R \times {}^0\mathbf{t}_F^C + \mathbf{d}_C^R]_{(3)}] \cdot \tilde{\mathbf{p}}_G^F \end{bmatrix}, \tag{33}$$

where $]_{(3)}$ indicates the third component of the vector, $\mathbf{d}_B^R$ and $\boldsymbol{\theta}_B^R$ define the DMV $\mathbf{x}_B^R$, and vectors ${}^0\mathbf{n}_j^i$, ${}^0\mathbf{o}_j^i$, ${}^0\mathbf{a}_j^i$ and ${}^0\mathbf{t}_j^i$ are defined for an HTM as

$${}^0\mathbf{H}_j^i = \begin{pmatrix} {}^0\mathbf{n}_j^i & {}^0\mathbf{o}_j^i & {}^0\mathbf{a}_j^i & {}^0\mathbf{t}_j^i \\ 0 & 0 & 0 & 1 \end{pmatrix}. \tag{34}$$

Since the RCS is the primary datum (A-CS), $\mathbf{x}_F^R$ has only 3 non-zero values in previous Eq. (33). For the fixture and part geometry given in Fig 4, the resolution of previous equation is

$$\begin{aligned} \mathbf{x}_F^R(2) &= -d_{Cz}^R + (p_{Gz}^F - t_{Fy}^C) \cdot \theta_{Cx}^R + (t_{Fx}^C - p_{Gx}^F) \cdot \theta_{Cy}^R \\ &\quad + p_{Gz}^F \cdot \theta_{Bx}^R, \end{aligned} \tag{35}$$
$$\mathbf{x}_F^R(3) = -d_{Bz}^R - t_{Fy}^B \cdot \theta_{Bx}^R + (p_{Ex}^F - t_{Fx}^B) \cdot \theta_{By}^R, \tag{36}$$
$$\mathbf{x}_F^R(4) = \theta_{Bx}^R, \tag{37}$$

where $\mathbf{p}_G^F = [t_{3x}^F, 0, t_{3z}^F]$ and the value of p_{Ex}^F is the parameter a which can be 0 or L_s depending on the fixture and part assembly.

Appendix B
Calculus of self-centering error due to single jaw deviations

Let us consider that the guiding slots of a 3-jaw self-centering chuck can be defined in a 2D plane as three lines which start from the coordinate origin, separated 120° to each other. Each jaw can be defined as a point located in each line, as it can be seen in Figure 13. In this nominal case, jaw P is located in the vertical line, with jaws Q and R named in clockwise order. Assuming a perfectly working chuck, all jaws are separated a distance G from the origin. Therefore, given a certain G, the position of each jaw in this ideal chuck with respect to the nominal FCS is

$$\begin{aligned} &(x_P, y_P) = (0, G), \\ &(x_Q, y_Q) = (-sin(30°) \cdot G, cos(30°) \cdot G), \\ &(x_R, y_R) = (-sin(30°) \cdot G, -cos(30°) \cdot G). \end{aligned}$$

A cylinder held by the chuck is represented in the 2D plane as a circumference tangent to points P, Q and R. If the jaws are perfectly self-centered, the center of the circumference will be located in the coordinate origin. However, these jaws may present a displacement from its self-centering position. For the sake of simplicity, the displacement, named δ, is applied to the single jaw P. By clamping the part under this jaw displacement, the following equations hold

$$(x_P, y_P) = (0, G + \delta), \tag{38}$$

$$(x_Q, y_Q) = (cos(30°) \cdot G, -sin(30°) \cdot G), \tag{39}$$

$$(x_R, y_R) = (-cos(30°) \cdot G, -sin(30°) \cdot G). \tag{40}$$

Given that the radius of the cylinder is *r* and that the circumference must be tangent to all three points, the distance from the center of the circumference to the coordinate origin expressed here as (x_C, y_C) can be calculated using the following equations

$$(x_P - x_C)^2 + (y_P - y_C)^2 = r^2, \tag{41}$$

$$(x_Q - x_C)^2 + (y_Q - y_C)^2 = r^2, \tag{42}$$

$$(x_R - x_C)^2 + (y_R - y_C)^2 = r^2. \tag{43}$$

Operating with previous equations we obtain

$$x_C^2 + y_C^2 - 2\delta y_C - 2G y_C + G^2 + 2G\delta + \delta^2 = r^2, \tag{44}$$

$$x_C^2 - \sqrt{3} G x_C + y_C^2 + G y_C + G^2 = r^2, \tag{45}$$

$$x_C^2 + \sqrt{3} G x_C + y_C^2 + G y_C + G^2 = r^2. \tag{46}$$

Solving these equations, we obtain that the deviation of the center x_C and y_C as

$$x_C = 0, \tag{47}$$

$$y_C = \frac{\delta^2 + 2\delta G}{2\delta + 3G}. \tag{48}$$

Finally, assuming that the displacement δ will be some orders of magnitude smaller than the value of the distance of the jaws to the center *G*, the previous equation can be approximated to

$$y_C = \frac{\delta^2 + 2\delta G}{2\delta + 3G} \approx \frac{2\delta G}{3G} = \frac{2}{3}\delta. \tag{49}$$

APPENDIX C
CALCULUS OF DATUM-INDUCED ERRORS IN 3-JAW SELF-CENTERING CHUCKS

In order to calculate matrix $\mathbf{A}_2$, let $\mathbf{p}_L$ be the locating pin that touches the secondary datum defined by B-CS in a 3-jaw chuck with configuration 1, as it is shown in Fig. 9. The nominal coordinates are defined as

$$\mathbf{H}_R^B \cdot \mathbf{H}_F^R \cdot \tilde{\mathbf{p}}_L^F = \tilde{\mathbf{p}}_L^B. \tag{50}$$

Additionally, the following expressions hold

$$\mathbf{H}_R^B = (\mathbf{H}_B^R)^{-1} = ({}^0\mathbf{H}_B^R \delta\mathbf{H}_B^R)^{-1} = \\ = (\delta\mathbf{H}_B^R)^{-1} \cdot {}^0\mathbf{H}_R^B = (\mathbf{I} - \mathbf{\Delta}_B^R) \cdot {}^0\mathbf{H}_R^B, \tag{51}$$

$$\mathbf{H}_F^R = {}^0\mathbf{H}_F^R \cdot (\mathbf{\Delta}_F^R + \mathbf{I}). \tag{52}$$

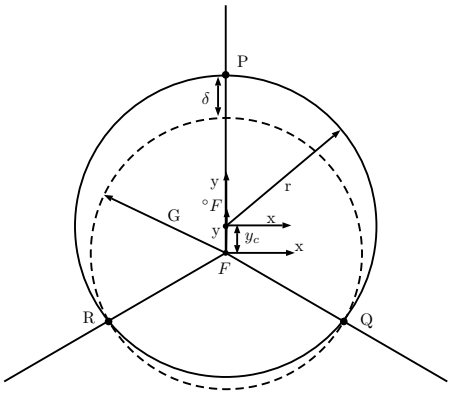

Fig. 13: Self-centering error y_C due to single jaw deviation δ. Dimensions of δ have been exaggerated to improve comprehension.

Therefore, substituting Eq. (51) and (52) in (50)

$$(\mathbf{I} - \mathbf{\Delta}_B^R) \cdot {}^0\mathbf{H}_R^B \cdot {}^0\mathbf{H}_F^R \cdot (\mathbf{\Delta}_F^R + \mathbf{I}) \cdot \tilde{\mathbf{p}}_L^F = \tilde{\mathbf{p}}_L^B. \tag{53}$$

Neglecting the second order terms

$$(-\mathbf{\Delta}_B^R \cdot {}^0\mathbf{H}_F^B + {}^0\mathbf{H}_F^B \cdot \mathbf{\Delta}_F^R + {}^0\mathbf{H}_F^B) \cdot \tilde{\mathbf{p}}_L^F \approx \tilde{\mathbf{p}}_L^B. \tag{54}$$

Considering that the 3 jaws and the locating points are perfect (no fixture errors), the locating point touches the secondary datum and thus, the Z coordinate of $\tilde{\mathbf{p}}_L^B$ is zero. Therefore,

$$\left[\left(- \mathbf{\Delta}_B^R \cdot {}^0\mathbf{H}_F^B + {}^0\mathbf{H}_F^B \cdot \mathbf{\Delta}_F^R + {}^0\mathbf{H}_F^B \right) \cdot \tilde{\mathbf{p}}_L^F \right]_{(3)} = 0. \tag{55}$$

Since locating pin touches the datum under nominal conditions, $\left[{}^0\mathbf{H}_F^2 \cdot \tilde{\mathbf{p}}_L^F \right]_{(3)} = 0$, then:

$$\left[\mathbf{\Delta}_B^R \cdot {}^0\mathbf{H}_F^B \cdot \tilde{\mathbf{p}}_L^F \right]_{(3)} = \left[{}^0\mathbf{H}_F^B \cdot \mathbf{\Delta}_F^R \cdot \tilde{\mathbf{p}}_L^F \right]_{(3)}. \tag{56}$$

We can rewrite the left hand of Eq. (56) as

$$[\mathbf{\Delta}_B^R \cdot {}^0\mathbf{H}_F^B \cdot \tilde{\mathbf{p}}_L^F]_{(3)} = \begin{bmatrix} [\boldsymbol{\theta}_B^R \times {}^0\boldsymbol{n}_F^B]_{(3)} \\ [\boldsymbol{\theta}_B^R \times {}^0\boldsymbol{o}_F^B]_{(3)} \\ [\boldsymbol{\theta}_B^R \times {}^0\boldsymbol{a}_F^B]_{(3)} \\ [\boldsymbol{\theta}_B^R \times {}^0\boldsymbol{t}_F^B + \mathbf{d}_B^R]_{(3)} \end{bmatrix}^T \cdot \tilde{\mathbf{p}}_L^F, \tag{57}$$

whereas the right hand of Eq. (56) is rewritten as

$$[{}^0\mathbf{H}_F^B \cdot \mathbf{\Delta}_F^R \cdot \tilde{\mathbf{p}}_L^F]_{(3)} = \begin{bmatrix} [{}^0\boldsymbol{a}_B^F]^T & [\mathbf{p}_L^F \times {}^0\boldsymbol{a}_B^F]^T \end{bmatrix} \cdot \mathbf{x}_F^R. \tag{58}$$

Solving Eq. (56) and reorganizing the terms, the deviation of the FCS w.r.t. RCS in Z axis direction is defined as

$$\mathbf{x}_F^R(3) = -d_{Bz}^R - p_{Lx}^F \cdot \theta_{By}^R - p_{Ly}^F \cdot \theta_{Bx}^R. \tag{59}$$

APPENDIX D
IMPLEMENTATION GUIDE TO PRACTITIONERS

In order to facilitate the industrial application of the SoV model based on workholding systems such as vices and 3-jaw chucks, we present the following step-by-step implementation guide. Please, note that the final purpose of this guide is to estimate part quality according to workholding specifications.

1) Identify the main key characteristics of the workholding systems to be used. For vices, parameters such as length and height of jaws (L_v, H_v) and contact width between support and workpiece (W_s). Additionally, position of primary, secondary and tertiary locating features (1-CS, 2-CS and 3-CS) w.r.t. FCS should be given. For 3-jaw chucks, parameters such as jaws position w.r.t. machine-tool $+Y$ direction (Ω), and locator position if exists (r_{loc} and θ_{loc}).
2) Build matrices $\mathbf{A}_k^2$ and $\mathbf{A}_k^3$ according to Eqs. (12), (18), (19) and Eqs. (21), (22), (27) for vices and 3-jaw chucks, respectively. In vices, these matrices will depend on the relationship between datum and fixture errors (i.e., matrices Γ_P and Γ_F).
3) Build the SoV model applying the methodology presented in Zhou et al. [4]. The SoV model requires the matrices previously derived $\mathbf{A}_k^2$ and $\mathbf{A}_k^3$. Include these matrices to obtain the SoV model in the form of Eq. (1).
4) Identify the technical specifications of the workholding systems provided by vendors. For vices, identify clamping accuracy, parallelism and perpendicularity of jaws; for 3-jaw chucks, identify maximum TIR (total indicator runout) in radial and axial direction and the dimensions of the part tested (diameter and length D_t and L_t) in the calibration sheet.
5) Run M Monte Carlo simulations constrained to previous technical specifications to generate M possible sets of fixture errors for each stage ($\mathbf{u}_k^F$). Eqs. (14), (15), (23) and (24) show some constrains for vices and 3-jaw chucks according to their technical specifications, so the generated data should be within them.
6) Apply the SoV model using the simulated fixture errors $\mathbf{u}_k^F$ to estimate the deviation of the inspected features from nominal values for the M simulations. An analysis of the deviations of the inspected features for the M simulations will show the capability of the process and the expected quality of the part.

REFERENCES

[1] Juanan Arrieta, Ander Azkarate, and Marcello Colledani. Zero defect manufacturing FR004. Roadmap. https://focusonfof.eu/downloads/results, 2016. Accessed: 2019-05-12.

[2] Jionghua Jin and Jianjun Shi. State Space Modeling of Sheet Metal Assembly for Dimensional Control. *Journal of Manufacturing Science and Engineering*, 1999.

[3] Dragan Djurdjanovic and Jun Ni. Dimensional Errors of Fixtures, Locating and Measurement Datum Features in the Stream of Variation Modeling in Machining . *Journal of Manufacturing Science and Engineering*, 125(4):716–730, 11 2003.

[4] Shiyu Zhou, Qiang Huang, and Jianjun Shi. State space modeling of dimensional variation propagation in multistage machining process using differential motion vectors. *IEEE Transactions on Robotics and Automation*, 19(2):296–309, 2003.

[5] Richard P Paul. *Robot manipulators: mathematics, programming, and control: the computer control of robot manipulators*. MIT Press, 1981.

[6] José V Abellán-Nebot, Jian Liu, F. Romero Subirón, and Jianjun Shi. State Space Modeling of Variation Propagation in Multistation Machining Processes Considering Machining-Induced Variations. *Journal of Manufacturing Science and Engineering*, 2012.

[7] Jaime Camelio, S. Jack Hu, and Dariusz Ceglarek. Modeling Variation Propagation of Multi-Station Assembly Systems With Compliant Parts. *Journal of Mechanical Design*, 125(4):673, 2003.

[8] Jean Philippe Loose, Shiyu Zhou, and Dariusz Ceglarek. Kinematic analysis of dimensional variation propagation for multistage machining processes with general fixture layouts. *IEEE Transactions on Automation Science and Engineering*, 4(2):141–151, 2007.

[9] J. Liu, J. Jin, and J. Shi. State space modeling for 3-d variation propagation in rigid-body multistage assembly processes. *IEEE Transactions on Automation Science and Engineering*, 7(2):274–290, April 2010.

[10] Tingyu Zhang and Jianjun Shi. Stream of Variation Modeling and Analysis for Compliant Composite Part Assembly— Part II: Multistation Processes. *Journal of Manufacturing Science and Engineering*, 138(12), jul 2016.

[11] José V. Abellán-Nebot, I. Peñarrocha, E. Sales-Setién, and J. Liu. Optimal inspection/actuator placement for robust dimensional compensation in multistage manufacturing processes. In J. Paulo Davim, editor, *Computational Methods and Production Engineering*, Woodhead Publishing Reviews: Mechanical Engineering Series, pages 31 – 50. Woodhead Publishing, 2017.

[12] D Djurdjanovic and J Ni. Online stochastic control of dimensional quality in multistation manufacturing systems. *Proceedings of the Institution of Mechanical Engineers, Part B: Journal of Engineering Manufacture*, 221(5):865–880, 2007.

[13] Yibo Jiao and Dragan Djurdjanovic. Compensability of errors in product quality in multistage manufacturing processes. *Journal of Manufacturing Systems*, 30(4):204–213, oct 2011.

[14] Jing Zhong, Jian Liu, and Jianjun Shi. Predictive control considering model uncertainty for variation reduction in multistage assembly processes. *IEEE Transactions on Automation Science and Engineering*, 7(4):724–735, 2010.

[15] L Eduardo Izquierdo, Jianjun Shi, S Jack Hu, and Charles W Wampler. Feedforward control of multistage assembly processes using programmable tooling. *Trans. NAMRI/SME*, 35:295–302, 2007.

[16] Ester Sales-Setién, Ignacio Peñarrocha-Alós, and José V Abellán-Nebot. Estimation of nonstationary process variance in multistage manufacturing processes using a model-based observer. *IEEE Transactions on Automation Science and Engineering*, 16(2):741–754, 2018.

[17] José V. Abellán-Nebot, Jian Liu, and F. Romero Subirón. Design of multi-station manufacturing processes by integrating the stream-of-variation model and shop-floor data. *Journal of Manufacturing Systems*, 30(2):70–82, 2011.

[18] Vincent Mckenna, Yan Jin, Adrian Murphy, Michael Morgan, Caroline Mcclory, Colm Higgins, and Rory Collins. Process selection using variation and cost relations. In *Advances in Manufacturing Technology XXX: Proceedings of the 14th International Conference on Manufacturing Research, Incorporating the 31st National Conference on Manufacturing Research, September 6–8, 2016, Loughborough University, UK*, volume 3, page 465. IOS Press, 2016.

[19] José V. Abellán-Nebot, Jian Liu, and F. Romero Subirón. Process-oriented tolerancing using the extended stream of variation model. *Computers in Industry*, 64(5):485–498, 2013.

[20] Yong Chen, Yu Ding, Jionghua Jin, and Dariusz Ceglarek. Integration of process-oriented tolerancing and maintenance planning in design of multistation manufacturing processes. *IEEE Transactions on Automation Science and Engineering*, 3(4):440–453, 2006.

[21] M Kamali Nejad, Frédéric Vignat, Alain Desrochers, and François Villeneuve. 3d simulation of manufacturing defects for tolerance analysis. *Journal of computing and information science in engineering*, 10(2), 2010.

[22] J.V. Abellán-Nebot and J. Liu. Variation propagation modelling for multi-station machining processes with fixtures based on locating surfaces. *International Journal of Production Research*, 51(15), 2013.

[23] José V Abellán-Nebot, Rubén Moliner-Heredia, Gracia M Bruscas, and J Serrano. Variation propagation of bench vises in multi-stage machining processes. *Procedia Manufacturing*, 41:906–913, 2019.

[24] Jeongmin Byun and C Richard Liu. Methods for improving chucking accuracy. *Journal of manufacturing science and engineering*, 134(5), 2012.

[25] Jean-Philippe Loose, Qiang Zhou, Shiyu Zhou, and Dariusz Ceglarek. Integrating GD&T into dimensional variation models for multistage machining processes. *International Journal of Production Research*, 48(11):3129–3149, 2010.

[26] Bryan R Fischer. *Mechanical tolerance stackup and analysis*. CRC Press, 2011.

[27] G Pahlitzsch and W Hellwig. The clamping accuracy of three-jaw chucks. In *Advances in Machine Tool Design and Research 1967*, pages 97–118. Elsevier, 1968.

[28] Jeongmin Byun and CR Liu. Selection of major locating surface for improving chucking accuracy. In *International Manufacturing Science and Engineering Conference*, volume 43628, pages 489–497, 2009.

Rubén Moliner-Heredia was born in Vila-real (Castelló), Spain in 1994. He received the M.Sc. degree in Industrial Engineering from the Universitat Jaume I de Castelló in 2018, and he is currently pursuing Ph.D degree in Industrial Technologies and Materials Program at Universitat Jaume I. His topics of interest are fault diagnosis and stream of variation in manufacturing systems.

José V. Abellán-Nebot is an Associate Professor in the Department of Industrial Engineering and Design at Universitat Jaume I de Castelló, Spain. He received his M.S. in Industrial Engineering and his Ph.D. in Technological Innovation Projects in Product and Process Engineering from the Universitat Jaume I de Castelló in 2003 and 2011, respectively. He was a Visiting Scholar at Monterrey Institute of Technology (2005), University of Michigan (2007), University of Arizona (2009 and 2012) and Georgia Institute of Technology (2014). His research interests focus on product quality due to the stream of variation in manufacturing systems and intelligent machining systems.

Ignacio Peñarrocha-Alós was born in Castelló, Spain in 1978. He received the M.Sc. degree in Industrial Engineering from the Universitat Jaume I de Castelló in 2002, and his Ph.D. in Computering and Control Engineering from Universitat Politècnica de València (UPV) in 2006. He has been working since 2004 at the Universitat Jaume I de Castelló. His current position is as an Associate Professor at the Department of Industrial Engineering and Design. He has participated in several local and national research projects. His research interests include identification, estimation, fault diagnosis and control over networks, and fault tolerant control of wind energy systems.